An allelic series of mutations in *Smad2* and *Smad4* identified in a genotype-based screen of *N*-ethyl-*N*-nitrosourea-mutagenized mouse embryonic stem cells

Jay L. Vivian*, Yijing Chen*, Della Yee, Elizabeth Schneider, and Terry Magnuson†

Department of Genetics, University of North Carolina, Chapel Hill, NC 27599

Edited by Richard D. Palmiter, University of Washington School of Medicine, Seattle, WA, and approved October 3, 2002 (received for review August 7, 2002)

Using selectable genes as proof of principle, a new high-throughput genotype-based mutation screen in mouse embryonic stem (ES) cells was developed [Chen *et al.* (2002) *Nat. Genet.* 24, 314–317]. If expanded to nonselectable genes, this approach would allow one to proceed quickly from sequence to whole-animal phenotypes. Here data are presented showing that a screen of a cryopreserved library of clonal, germ line competent, *N*-ethyl-*N*-nitrosurea (ENU) mutagenized ES cells can identify a large series of allelic mutations in *Smad2* and *Smad4*, two nonselectable genes of the transforming growth factor β superfamily of signaling molecules. Whole animal phenotypic analyses of some of these alleles provided evidence for novel developmental processes mediated by these components of transforming growth factor β signaling, demonstrating the utility of non-null alleles created by chemical mutagens. The accurately assessed mutation load of the ES cell library indicates that it is a valuable resource for developing mouse lines for genetic and functional studies. This methodology can conceptually be applied for the generation of an allelic series of subtle mutations at any locus of interest in the mouse.

Allelic series of mutations in the mouse produced by chemical mutagens such as *N*-ethyl-*N*-nitrosourea (ENU) are valuable reagents to reveal a full spectrum of gene functions *in vivo*. Non-null alleles are useful in particular, as they allow for fine-tuned analysis of later functions of genes whose null allele results in lethality and for investigation of protein domains through isolated disruption of specific amino acid residues. The efficiency of ENU as a mutagen has made it the mutagen of choice in whole animal phenotype-based screens (1). Recently, experiments have shown that mutations in specific genes of interest can be obtained by screening DNA derived from mutagenized mice and reconstituting the mouse line from cryopreserved sperm (2). However, the large number of mice required to identify multiple mutations in any given gene with whole-animal mutagenesis may be prohibitive, thus more efficient gene-based methods will be needed to produce large numbers of subtle mutations in the mouse. We and others have shown that mouse embryonic stem (ES) cells can be efficiently mutagenized with chemical mutagens at several selectable loci, while retaining their ability to populate the germ line (3, 4). If this methodology could be extended to identify ES cells with mutations in specific genes of interest, one could then quickly proceed from gene sequence to developing a large allelic series of mutations in the mouse.

Smad2 and *Smad4* are vertebrate members of the Smad family of intracellular transducers of transforming growth factor β (TGF-β) superfamily signaling (5). Current models posit *Smad2* to be a receptor-regulated-Smad activated via phosphorylation in response to ACTIVIN, TGF-β, and NODAL signaling. *Smad4* is the only known mammalian common-mediator Smad that interacts with receptor-regulated Smads after their activation. This Smad complex then translocates to the nucleus to effect transcription of target genes through direct interaction with a variety of other transcriptional regulators. The modulation of TGF-β signaling pathway by other signaling pathways, such as the mitogen-activated protein kinase pathways, is in part mediated by phosphorylation sites within the linker domain of receptor-regulated Smads (6, 7). Targeted disruption of either the murine *Smad2* or *Smad4* genes results in a peri-gastrulation lethality (8). These mutants have uncovered functions of these factors in a variety of developmental processes, including epiblast profileration, mesoderm formation, and extraembryonic tissue-mediated early embryonic patterning events (8). However, the requirements for these factors in later embryonic development and adult life remain largely unknown. Hypomorphic alleles that bypass the early embryonic requirement for *Smad2* and *Smad4* would be useful tools to analyze the functions of these factors in later life. Additionally, the importance of the various protein interactions and posttranslational modification sites in SMAD2 and SMAD4 can be analyzed *in vivo* with point mutations that specifically disrupt these protein domains.

We describe here the isolation of a large allelic series of mutations in *Smad2* and *Smad4* by combining ENU mutagenesis of mouse ES cells with high throughput mutation detection technology. Phenotypic analyses of some of these mutations in the mouse, including a hypomorphic allele of *Smad2* and a splice mutant allele of *Smad4*, revealed previously undescribed functions of these factors. These allelic series of mutations in *Smad2* and *Smad4* will serve as useful genetic tools for studying biological processes mediated by *Smad2* and *Smad4*. The methodology can be applied to most genes to develop an allelic series of mutations in the mouse, facilitating the functional annotation of the mammalian genome.

Materials and Methods

ES Cell Culture and Mutagenesis. CT129 ES cells (9) were cultured as described. The cells were grown for two passages without feeders before ENU treatment. After the second passage onto gelatin-coated plates, the cells were incubated with 0.2 mg/ml ENU (Sigma) in culture medium for 2 h. The cells were then washed, trypsinised, and plated at the appropriate density to allow formation of individual colonies. Colonies were picked into gelatin-coated 96-well plates, grown, and split in duplicate. A total of 2,060 ES cells were picked from three separate mutagenesis experiments. One plate was cryopreserved as a mutagenized cell bank; the other plate was used to prepare total RNA and genomic DNA (Qiagen, Valencia, CA) for mutation detection.

Mutation Detection. Total RNA from ENU-mutagenized ES cell clones was isolated for use in an RT-PCR-based amplification of

This paper was submitted directly (Track II) to the PNAS office.

Abbreviations: ENU, *N*-ethyl-*N*-nitrosourea; TGF-β, transforming growth factor β; ES, embryonic stem; PECAM, platelet-endothelial cell adhesion molecule.

*J.L.V. and Y.C. contributed equally to this work.

†To whom correspondence should be addressed. E-mail: trm4@med.unc.edu.

the coding regions of mouse *Smad2* and *Smad4*. Oligonucleotides specific to *Smad2* or *Smad4* were used to amplify overlapping amplicons to cover the entire coding regions of these genes (Table 4, which is published as supporting information on the PNAS web site, www.pnas.org). PCR products were denatured and annealed immediately after PCR in the thermocycler. Denaturing high performance liquid chromatography (DHPLC)-based heteroduplex analysis of the PCR products was performed by the WAVE fragment analysis system (Transgenomic, Omaha, NE) using UV absorbance for detection. Optimal DHPLC conditions for each amplicon were identified by analysis of point mutations created by *in vitro* mutagenesis. ES cell clones harboring candidate mutations were thawed and expanded, and RNA was isolated for RT-PCR. Presence of the mutation was confirmed by heteroduplex analysis as above. The base change of each mutation was identified by direct sequencing of the PCR product.

Generation of Mice. ES cell lines harboring identified point mutations were thawed from their multiwell array and expanded. To assess whether each line was clonal, a subcloning procedure was performed. In brief, each ES cell line was grown and trypsinized, and single ES cells were picked by mouth pipette using a microscope and seeded onto feeders. After 7 days, 40 single cell colonies on these plates were picked into a multiwell plate and subsequently split for cryopreservation and RNA isolation. RNA was used for RT-PCR amplification and WAVE analysis as described. If all ES cell subclones of a given line were identified as carrying the point mutation, then the nonsubcloned parental line was used for injection; otherwise pools of three single-cell subclones carrying the point mutation were used for injection into blastocysts.

Blastocyst injections for production of chimeric mice were performed by standard procedures. Chimeras were mated to wild-type C57BL/6 or Black Swiss mice for testing germ-line transmission. Germ-line transmission was assessed by coat color and by genotyping with genomic DNA from tail biopsy. Genotyping was performed by heteroduplex analysis of PCR products amplifying the genomic region spanning the point mutation. Mouse stocks were maintained in the heterozygous state by crossing heterozygous mice to wild-type mice of the desired background for multiple generations.

Mouse Breeding. To obtain mice carrying an ENU-induced point mutation within *Smad2* or *Smad4* over a targeted allele, mice heterozygous for a point mutation were crossed to heterozygous mice for targeted alleles of *Smad2* (10) or *Smad4* (11). Pups or embryos were genotyped by using tail- or yolk sac-derived DNA,

Table 1. Summary of ENU-induced mutations in *Smad2* and *Smad4*

Gene	Allele	ES cell clone	Nucleotide change*	Codon change	Exon	Amino acid change	Region of protein†
Smad2		LM1-2G2	T523A	CTG to CAG	4	L155Q	MH1 turn 5
		LM2-2A6	A1411G	AAA to AGA	11	K451R	MH2 domain, H5
		LM2-2E8	G1205T	CTG to CTT	10	Silent L382	
		LM2-3B1	T781C	ATG to ACG	6	M241T	Linker, CaM kinase II phosphorylation motif (30)
	m1Mag	LM2-3F6	C886T	TCA to TTA	8	S276L	MH2, B1 sheet
		LM2-4A4	A719G	ACA to ACG	6	Silent T220	
		LM2-4H1	C183G	CAA to GAA	2	Q41E	MH1 helix 2, calmodulin binding domain (31)
		LM2-7D9	T792G	TCT to GCT	7	S245A	Linker, putative proline-directed kinase site (7)
		LM2-8C9	A1059G	AGG to GGG	8	R334G	MH2, B5 sheet
		LM3-1D6	T818C	ACT to ACC	7	Silent T253	
		LM3-2H10	T1129A	ATC to AAC	9	I355N	MH2, between B6 and B7 sheets
		LM3-5A6	SA −7 T→G	NA	Int 2	RN insertion after P78	MH1, adjacent to SMAD2 unique region
		LM3-5E7	C718G	ACA to AGA	6	T220K	Linker, putative ERK phosphorylation site (7)
Smad4							
	m3Mag	LM1-1H11	G1467A	GGC to AGC	9	G383S	MH2, B5 sheet
		LM1-1H2	T1228C	CAT to CAC	7	Silent H316	
		LM1-2H8	C812T	GAC to GAT	4	Silent D164	
		LM2-5B6	T1945A	ATG to AAG	11	M542K	MH2, H5
		LM2-9F5	C1529T	GAC to GAT	9	Silent D403	
		LM3-10D7	C340T	ACA to ATA	1	T7I	Just N′ to MH1
		LM3-10E2	A1588G	GAC to GGC	9	D423G	MH2, between H2 and B8
	m4Mag	LM3-1A5	SD +1 G→A	Exon 10 deletion	Int10	aa436+19 out of frame aa	Deletion of QA insert and the rest of MH2
	m1Mag	LM3-1A6	T362A	GAT to GAA	1	D14E	Just N′ to MH1
		LM3-1G1	C1607T	TAC to TAT	9	Silent Y429	
		LM3-2E3	C1920T	CTC to TTC	11	L534F	MH2, H5
		LM3-3D1	C1222T	TAC to TAT	6	Silent Y300	
		LM3-3F5	C346A	ACA to AAA	1	T9K	Just N′ to MH1
	m2Mag	LM3-4C12	A858G	ACC to GCC	4	T180A	Linker, high homology with *Medea* (32)
		LM3-7C5	C803T	TAC to TAT	4	Silent Y161	
		LM3-7D6	C1215T	CAT to TAT	6	H299Y	Linker, p300 binding, transactivation domain (33)

SA, splice acceptor; SD, splice donor; Int, intron; MH, Mad homology; NA, not applicable.
*Data are from refs. 28 and 29.
†Data are from refs. 25 and 29 unless otherwise noted.

Table 2. Mutation frequencies at *Smad2* and *Smad4* loci

	Total base pairs screened, Mb	No. of mutations identified	ES cell clone mutation frequency	Nonsilent ES cell mutation frequency	Per-base mutation frequency, kb	Nonsilent per-base mutation frequency, kb
Smad2	6.06	13	1 in 158	1 in 206	1 in 466	1 in 606
Smad4	7.40	16	1 in 129	1 in 206	1 in 463	1 in 740
Overall	13.46	29	1 in 143	1 in 206	1 in 464	1 in 673

using PCR-based methods to detect the targeted alleles as described, and heteroduplex formation to detect the presence of the point mutations (Table 5, which is published as supporting information on the PNAS web site). Intercrosses of mice heterozygous for a point mutation were performed to obtain mice homozygous for that mutation. Genotyping was accomplished by heteroduplex analysis. Homozygous wild-type and homozygous mutant PCR samples were distinguished by mixing an equimolar amount of wild-type control PCR product, annealed and subjected to heteroduplex detection.

Histology and Immunochemistry. Embryos were fixed overnight in 4% paraformaldehyde, then washed in PBS. Platelet-endothelial cell adhesion molecule (PECAM) was detected in whole embryos with an anti-PECAM antibody (PharMingen) as described (12). Sectioning was performed by paraffin embedding and staining with nuclear fast red or hematoxylin and eosin.

Western Blotting. The ES cells were lysed on ice for 30 min in buffer containing 50 mM Tris (pH 7.4), 0.5% Nonidet P-40, 0.25% sodium deoxycholate, 150 mM NaCl, 1 mM EGTA, and protease inhibitors (Roche). The lysate was cleared of debris by centrifugation. The total protein concentration was measured by using the Coomassie Plus Protein Assay Reagent (Pierce). Equal amounts of protein were separated on a SDS/10% PAGE gel and transferred to poly(vinylidene difluoride) membranes (Millipore). The SMAD4 protein was detected by using the B-8 monoclonal antibody (Santa Cruz Biotechnology). A polyclonal anti-ACTIN antibody (I-19, Santa Cruz Biotechnology) was used as a control for equal loading.

Results

Identification of ENU-Induced *Smad2* and *Smad4* Mutations. To screen for ES cells with mutations in specific genes of interest, a cryopreserved library of mutagenized ES colonies was developed by using a slightly modified method of ENU treatment from what we described (3). A total of 2,060 mutagenized ES cell clones were cryopreserved from three separate experiments in a 96-well format to facilitate subsequent processing procedures. Total RNA and genomic DNA were isolated from individual mutagenized lines. Because both *Smad2* and *Smad4* are expressed in ES cells, RT-PCR was performed to amplify overlapping segments covering the entire coding regions of both genes. When a denaturing high performance liquid chromatography-based heteroduplex detection scheme was used (13), a total of 29 ES cell clones were identified with mutations in *Smad2* or *Smad4* (Table 1). All mutations were single nucleotide substitutions, which is consistent with the known mutagenic properties of ENU (14). Eighteen mutations (62%) resulted in missense alterations of the protein. Two mutations affected splicing through alterations in intronic sequences at the splice junctions (15). The remaining mutations (31%) were silent. The mutation frequencies of *Smad2* and *Smad4* were remarkably similar with an overall mutation rate of 1 in 464 kb and an average nonsilent mutation rate of 1 in 673 kb (Table 2).

Thirteen karyotypically normal cell lines carrying nonsilent mutations were expanded for injection into blastocysts to create chimeric mice for germ-line transmission of the ENU-generated mutations. Consistent with our earlier work (3), mutagenized ES cells readily made germ line competent chimeras. Five mutations have been passed through the germ line. Complementation tests were performed by crossing each mutation against a correspond-

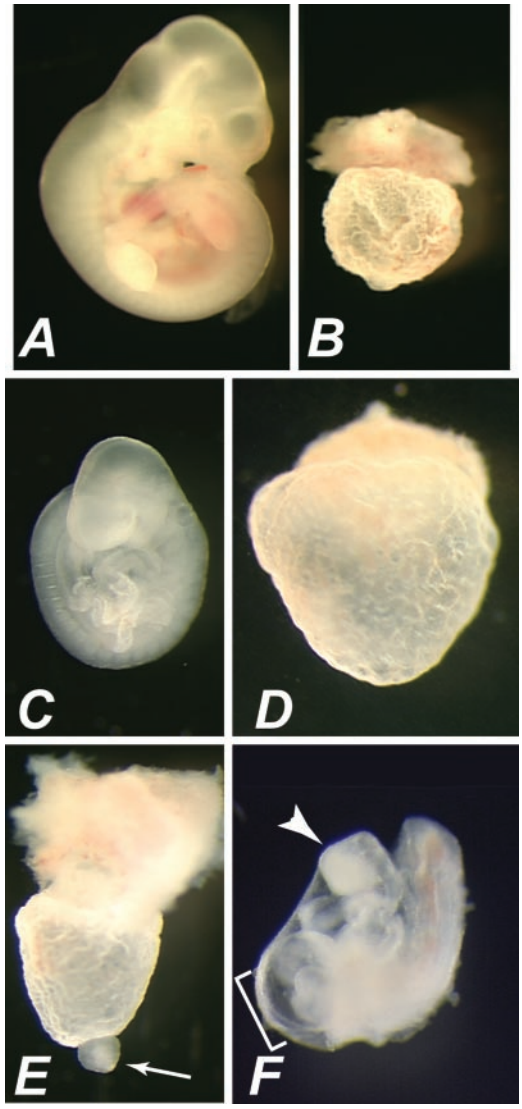

Fig. 1. Severe embryonic defects associated with $Smad2^{m1Mag}$ mutation. (*A* and *B*) Gross morphology of wild-type (*A*) and $Smad2^{m1Mag}/Smad2^{Robm1}$ (*B*) concepti at E11.5. $Smad2^{m1Mag}/Smad2^{Robm1}$ concepti consist of an empty yolk sac devoid of an embryo proper. (*C*) Wild-type embryo at E9.5. (*D–F*) Three classes of $Smad2^{m1Mag}/Smad2^{m1Mag}$ embryos at E9.5. (*D*) The empty yolk sac closely resembles the phenotype observed in $Smad2^{m1Mag}/Smad2^{Robm1}$ (*B*). (*E*) A mass of tissue at the distal tip (arrow) is observed in another class of $Smad2^{m1Mag}/Smad2^{m1Mag}$ embryo. This mass of tissue is contractile, indicating the presence of some cardiac muscle differentiation. (*F*) The most advanced class of $Smad2^{m1Mag}/Smad2^{m1Mag}$ embryo exhibits many embryonic structures. Note the expanded pericardial cavity (bracket) and truncated anterior neurectoderm (arrowhead).

Table 3. Complementation tests with targeted alleles (KO)

ENU allele*	+/+	ENU/+	+/KO	ENU/KO	Total
Smad2^{m1Mag}	14	6	8	0 (4)†	32
Smad4^{m1Mag}	14	15	6	6	41
Smad4^{m2Mag}	22	20	19	21	82
Smad4^{m3Mag}	14	18	19	18	69
Smad4^{m4Mag}	14	16	17	0	47

**Smad2* analysis was performed at E9.5 to E11.5. *Smad4* analysis was performed at postnatal stages.
†All *Smad2*^{m1Mag}/*Smad2*^{Robm1} concepti consisted of an empty yolk sac.

ing targeted mutation in addition to crossing each mutation to homozygosity. A range of phenotypes was observed in mice derived from these crosses.

***Smad2*^{m1Mag} Is a Hypomorphic Allele.** One ENU-induced allele, *Smad2*^{m1Mag}, changed a serine to leucine in amino acid 276 within the edge of the Mad homology 2 domain. This serine residue is conserved amongst all vertebrate and most invertebrate receptor-regulated Smads, suggesting an important structural function of this precise region of the protein. However, no protein interactions have been localized to this region of SMAD2, nor has there been any report of serine-276 to be phosphorylated. Early embryonic defects were observed when the *Smad2*^{m1Mag} allele was placed against a targeted allele of *Smad2*, *Smad2*^{Robm1} (10). Although *Smad2*$^{+}$/*Smad2*^{m1Mag} littermates were normal at 11.5 days of gestation (E11.5, Fig. 1*A*), a highly developed yolk sac devoid of any embryonic portion was observed in *Smad2*^{m1Mag}/*Smad2*^{Robm1} heterozygotes (Table 3, Fig. 1*B*). Yolk sac blood islands were apparent, consistent with extraembryonic mesoderm formation. These phenotypes closely resemble those observed in homozygous *Smad2*^{Robm1} embryos and indicate a substantial loss of function associated with the *Smad2*^{m1Mag} allele.

At E9.5 (Fig. 1 *C–F*), some homozygous *Smad2*^{m1Mag} embryos consisted of an empty yolk sac, resembling *Smad2*^{m1Mag}/*Smad2*^{Robm1} and *Smad2*^{Robm1}/*Smad2*^{Robm1} embryos (54%, n = 34, Fig. 1*D*), though occasionally a malformed embryonic structure was present at the distal portion of the yolk sac (Fig. 1*E*). However, many *Smad2*^{m1Mag} homozygous embryos (46%) exhibited considerably more advanced development. These embryos displayed obvious epiblast-derived structures, including a heart, tail bud, allantois, and somites (Fig. 1*F*). The allantois of these embryos failed to fuse to the chorion, resulting in allantoic tissue protruding from the posterior of the embryo (not shown). Severe anterior patterning defects were also observed in these *Smad2*^{m1Mag} homozygous embryos. Anterior structures consisted of a truncated mass often with an unfolded neural plate, and the optic placode was not apparent. Although anterior midline tissues were morphologically apparent in wild-type embryos at E8.5 (Fig. 2 *A* and *C*), the absence of an anterior notochord and a small or absent foregut were observed in *Smad2*^{m1Mag} homozygotes (Fig. 2 *B* and *D*). The advanced embryonic development of *Smad2*^{m1Mag}/*Smad2*^{m1Mag} embryos compared with that of the targeted alleles of *Smad2*, including the ability to form many embryonic tissues, strongly suggested that *Smad2*^{m1Mag} is a hypomorph.

Vascular Defects in *Smad2*^{m1Mag} Mutant Embryos. *Smad2*^{m1Mag} homozygous embryos with fused heart tubes displayed an expanded pericardial cavity (Fig. 1*F*) and erratic cardiac contractility, suggesting that cardiovascular defects may cause the embryonic lethality observed in these embryos after E9.5. Because vascular defects have been observed in several mutants of other TGF-β signaling components (16), the early embryonic vasculature was visualized with an anti-PECAM antibody. Although endothelial cells were present in both wild-type and mutant embryos (Fig. 2 *E* and *F*), the dorsal aorta in these *Smad2*^{m1Mag} homozygotes was either highly constricted or lacked an aortic lumen present at this time in wild-type embryos (Fig. 2 *G* and *H*) and was generally more severe in the anterior of the embryo. The defects observed in *Smad2*^{m1Mag} homozygous embryos confirmed the requirement for *Smad2* in the proper formation of the anterior neurectoderm and foregut and demonstrate a function for *Smad2* in chorioallantoic fusion and vascular development.

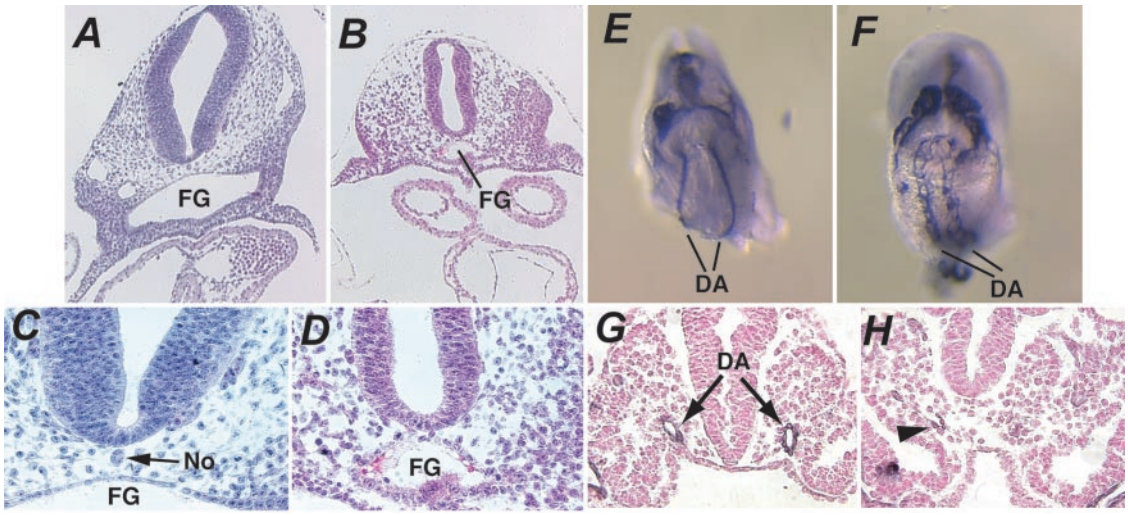

Fig. 2. Defects in the formation of the dorsal aorta, foregut, and notochord in *Smad2*^{m1Mag}/*Smad2*^{m1Mag} embryos. (*A–D*) Hematoxylin and eosin staining of transverse histological sections of wild-type (*A* and *C*) and *Smad2*^{m1Mag}/*Smad2*^{m1Mag} (*B* and *D*) embryos at E9.5 about the level of the heart at ×10 (*A* and *B*) and ×20 (*C* and *D*) objective magnification. *Smad2*^{m1Mag}/*Smad2*^{m1Mag} embryos display a small foregut (FG) compared with wild type and lack a morphologically obvious notochord (No). (*E* and *F*) Ventral view of the dorsal aortae (DA) at the region of the opening of the foregut of intact wild-type (*E*) and *Smad2*^{m1Mag}/*Smad2*^{m1Mag} (*F*) embryos at E8.5 visualized with an anti-PECAM antibody. Significant endothelial differentiation is observed in mutant embryos but the aorta fails to condense fully. (*G* and *H*) Transverse sections of PECAM-stained embryos at the level of the foregut entrance of wild-type (*G*) and *Smad2*^{m1Mag}/*Smad2*^{m1Mag} (*H*) embryos at E8.5. The cells of the dorsal aortae display strong PECAM expression about the aortic lumen in wild-type embryos. Although PECAM-positive endothelial cells are present in mutant embryos (*H*, arrowhead), cells fail to form an aortic lumen in this region of the embryo.

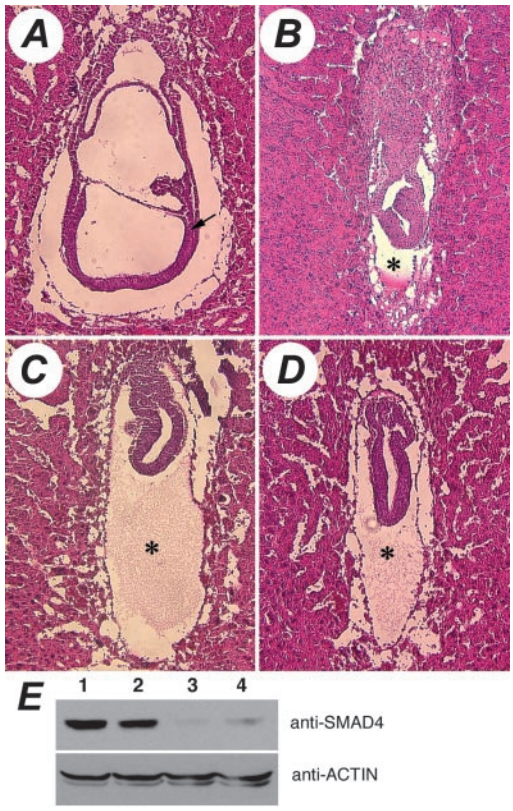

Fig. 3. Defects associated with the *Smad4*^{m4Mag} allele. Hematoxylin and eosin-stained sagittal sections of E7.5 embryos are shown. (*A*) Wild-type gastrulating embryo showing newly formed mesoderm (arrow) and other well patterned structures. (*B*) Homozygous *Smad4*^{tm1Cxd} embryo. (*C*) *Smad4*^{m4Mag}/*Smad4*^{tm1Cxd} embryo. (*D*) Homozygous *Smad4*^{m4Mag} embryo. (*B–D*) Compared with the wild-type E7.5 embryo (*A*), these mutant embryos are much smaller, with no sign of the initiation of gastrulation or the formation of mesoderm. Also note the disproportionally large cavity between the visceral and parietal endoderm (asterisks). (*E*) Steady-state level of SMAD4 protein in unmutagenized wild-type ES cells (lane 1) and three mutagenized sibling subclones (lane 2, wild-type for *Smad4*; lanes 3 and 4, heterozygous for *Smad4*^{m4Mag}). The same blot was stripped and reprobed with an anti-ACTIN antibody to show equal loading of total cellular proteins.

Viability of Several ENU-Induced *Smad4* Alleles. Three of the four ENU-induced *Smad4* alleles (*Smad4*^{m1Mag}, *Smad4*^{m2Mag}, and *Smad4*^{m3Mag}) resulted in missense substitutions of conserved amino acid residues (Table 1). Surprisingly, animals carrying each of these mutations survived to adulthood either in combination with the targeted *Smad4*^{tm1Cxd} allele (17) or in the homozygous state (Table 3), indicating that these missense substitutions do not significantly perturb the functions of the SMAD4 protein during embryogenesis. To date, these animals have been aged for at least 5 months, and no overt phenotypes have been observed either in the compound heterozygotes or homozygotes.

***Smad4*^{m4Mag} Is a Splice Mutant Allele.** The fourth *Smad4* allele, *Smad4*^{m4Mag}, altered a conserved nucleotide in the splice donor of the intron 10, causing the deletion of exon 10. This aberrant transcript is predicted to produce a truncated protein with an additional 19 out-of-frame amino acids after amino acid 436 in the highly conserved Mad homology 2 domain. Consistent with the drastic alteration in the gene product, mice that are compound heterozygous for the *Smad4*^{m4Mag} allele and the targeted allele *Smad4*^{tm1Cxd} did not survive embryogenesis (Table 3). Compared with the wild-type E7.5 embryo (Fig. 3*A*), these animals were severely growth-retarded, failed to initiate gastrulation and consequently did not form mesoderm (Fig. 3*C*). Animals homozygous for *Smad4*^{m4Mag} displayed similar phenotypes (Fig. 3*D*) and closely resembled those of the *Smad4*^{tm1Cxd} homozygotes (Fig. 3*B*), indicating a severe loss of function associated with the *Smad4*^{m4Mag} allele. However, examination of the steady-state SMAD4 protein levels in *Smad4*^{m4Mag} heterozygous ES cells revealed that *Smad4*^{m4Mag} is not a conventional null allele. Wild-type SMAD4 protein levels in the *Smad4*^{m4Mag} heterozygous ES cell lines were dramatically lower than the expected level of 50% (Fig. 3*E*). Additionally, no truncated mutant SMAD4 protein, predicted to be 51 kDa, was detected. Similar reduction of the wild-type SMAD4 protein level as well as the absence of the truncated protein was also seen in primary embryonic fibroblasts of *Smad4*^{m4Mag} heterozygotes (data not shown). The reduction of wild-type protein indicates that not only is the truncated mutant protein unstable, it possibly confers instability to the wild-type protein as well in heterozygous cells, suggesting a dominant negative property of the *Smad4*^{m4Mag} allele.

Discussion

Our results demonstrate that combining chemical mutagenesis in mouse embryonic stem cells with high throughput mutation detection allows for the rapid identification of subtle mutations in nonselectible genes of interest. A variety of alleles can be quickly obtained in a modest sized genotype-based screen. Thus far we have obtained three viable alleles (*Smad4*^{m1Mag}, *Smad4*^{m2Mag}, *Smad4*^{m3Mag}), a hypomorphic allele (*Smad2*^{m1Mag}), and an allele (*Smad4*^{m4Mag}) that resembles the null allele in the homozygous state but acts molecularly as a dominant negative in the heterozygous state.

Assessment of Mutation Load in Genotype-Based Screens. Although predictions of mutation load have been attempted from whole animal phenotype-based screens (18), only with the recent introduction of genotype-based screens in the mouse has a per-base assessment of mutation load been possible (2, 18). However, highly differing numbers have been reported because of differences in sample size, the mutagen dose and the sensitivity of the mutation identification methods. The large sample size of our screen and consistent mutation frequencies between two independent loci indicate an accurate assessment of mutation load in our cryopreserved bank. With a mutation frequency of 1 in 464 kb, the average distribution of nonsilent coding sequence variations in this ES cell library is ≈1 per 13 centimorgans (cM), assuming a 1,600-cM, 2.7 Gb haploid mouse genome of which 3% is coding. Thus, the ES cell library is a useful reagent for developing mouse lines carrying mutations at specific loci. It is worth noting that a similar mutation frequency of 1 sequence variation per 482 kb was observed in a genotype-based screen in zebrafish exposed to a dose of ENU typically used in phenotype-driven screens (19). If desired, mutagenesis procedures can be readily altered in cell culture to lower mutation load, taking advantage of the ability to monitor the mutation load of a cryopreserved library in culture with selectable loci. Phenotypic analysis of mutations obtained in any chemical mutagenesis would be best analyzed by using compound heterozygotes, possibly by using alleles with similar phenotypic severity, which requires multiple mutant alleles of a gene. The high throughput nature of the ES-cell-based genotypic screen allows for the rapid development of such allelic series of mutations.

***Smad2*^{m1Mag} Is a Tool to Analyze *Smad2* Function in Embryonic Development.** The *Smad2*^{m1Mag} allele demonstrates the utility of subtle mutations for uncovering previously uncharacterized gene function. Owing to the advanced development of some of these

mutants, the ENU induced *Smad2*^{m1Mag} allele suggests requirements for *Smad2* not revealed in any *Smad2* targeted mutation, including functions in chorioallantoic fusion and cardiovascular development. Additionally, this allele confirms functions for *Smad2* in anterior development and endoderm formation (20, 21). The less severe class of *Smad2*^{m1Mag} homozygous embryos is likely due to a partial or full rescue of the requirement of *Smad2* in extraembryonic tissues to pattern the epiblast (10), suggesting that the mouse embryo must be highly sensitive to threshold levels of TGF-β-related signaling in extraembryonic tissues to mediate early embryo patterning. The distinct phenotypic classes of defects observed in *Smad2*^{m1Mag} homozygotes resemble those observed in a hypomorphic allele of *nodal*, confirming the requirement for *Smad2* in mediating NODAL signaling in a variety of embryonic stages (20).

Mutations in several other components of TGF-β signaling result in defects in vascular development, including *Alk1*, *Smad5*, and *TGF-β1*, which have similar phenotypes, including an enlarged dorsal aorta (16). The failure of normal dorsal aorta formation in *Smad2*^{m1Mag} homozygotes appears phenotypically different from these mutations, suggesting that the *Smad2*^{m1Mag} allele has uncovered potentially novel aspects of TGF-β-related signaling in vascular development. One intriguing possibility is that the notochord or foregut defects observed in *Smad2*^{m1Mag} homozygotes underlie the vascular defects in these embryos. The failure of endoderm formation in *Smad2*^{m1Mag} homozygotes is consistent with previous data showing that *Smad2*-deficient cells do not efficiently contribute to the definitive endoderm lineage (21). The *Smad2*^{m1Mag} allele will thus provide a useful tool to analyze *Smad2*-mediated endoderm development, as well as the functional consequences of loss of endoderm-derived tissues in the early embryo.

SMAD4 Truncation Mutations and Dominant Negative Activities. Several studies have shown that C-terminal truncations of the SMAD4 protein display dominant negative properties (22, 23) or are highly unstable and rapidly degraded via the ubiquitin-proteasome pathway (24). Although the *Smad4*^{m4Mag} splice mutation deletes the C-terminal helix bundle thought to be important for homo-oligomerization (25), its intact Mad homology 1 domain, the linker region, and the remaining Mad homology 2 domain may be sufficient for oligomerization with the wild-type SMAD4 protein. Similar C-terminal truncations of SMAD4 protein have been shown to retain their ability to interact with the full-length wild-type protein (26). As cellular SMAD4 is found mostly in a homo-oligomer state (27), the decreased wild-type SMAD4 protein in the *Smad4*^{m4Mag} heterozygous cells could be due to the association of mutant protein with the wild-type protein, which is then targeted for degradation. It is remarkable that the heterozygous ES cells and animals are phenotypically normal despite the low levels of SMAD4 protein, suggesting a low threshold level of SMAD4 protein required for normal development and function in the cell and tissue types examined. The nonallelic, noncomplementation of some of the receptor-regulated Smads (28) underscores the dosage sensitive aspect of the TGF-β-related signaling. The apparent dominant negative property of the *Smad4*^{m4Mag} allele and hypomorphic nature of the *Smad2*^{m1Mag} allele will provide unique sensitized backgrounds both *in vitro* and *in vivo* for studying the importance of these factors in various biological processes.

We thank E. Robertson and X. Deng for providing *Smad2* and *Smad4* targeted mice, respectively. This work was supported by National Institutes of Health postdoctoral fellowships (to J.L.V. and Y.C.), an American Heart Association postdoctoral fellowship (to J.L.V.), and a National Institutes of Health grant (to T.M.).

1. Russell, W. L., Kelly, E. M., Hunsicker, P. R., Bangham, J. W., Maddux, S. C. & Phipps, E. L. (1979) *Proc. Natl. Acad. Sci. USA* **76,** 5818–5819.
2. Coghill, E. L., Hugill, A., Parkinson, N., Davison, C., Glenister, P., Clements, S., Hunter, J., Cox, R. D. & Brown, S. D. (2002) *Nat. Genet.* **30,** 255–256.
3. Chen, Y., Yee, D., Dains, K., Chatterjee, A., Cavalcoli, J., Schneider, E., Om, J., Woychik, R. P. & Magnuson, T. (2000) *Nat. Genet.* **24,** 314–317.
4. Munroe, R. J., Bergstrom, R. A., Zheng, Q. Y., Smith, R., John, S. W., Schimenti, K. J., Libby, B. J., Browning, V. L. & Schimenti, J. C. (2000) *Nat. Genet.* **24,** 318–321.
5. Attisano, L. & Tuen Lee-Hoeflich, S. (2001) *Genome Biol.* **2,** 3010.1–3010.8.
6. Kretzschmar, M., Liu, F., Hata, A., Doody, J. & Massagué, J. (1997) *Genes Dev.* **11,** 984–995.
7. Kretzschmar, M., Doody, J., Timokhina, I. & Massague, J. (1999) *Genes Dev.* **13,** 804–816.
8. Weinstein, M., Yang, X. & Deng, C. (2000) *Cytokine Growth Factor Rev.* **11,** 49–58.
9. Threadgill, D. W., Yee, D., Matin, A., Nadeau, J. H. & Magnuson, T. (1997) *Mamm. Genome* **8,** 390–393.
10. Waldrip, W. R., Bikoff, E. K., Hoodless, P. A., Wrana, J. L. & Robertson, E. J. (1998) *Cell* **92,** 797–808.
11. Sirard, C., de la Pompa, J. L., Elia, A., Itie, A., Mirtsos, C., Cheung, A., Hahn, S., Wakeham, A., Schwartz, L., Kern, S. E., *et al.* (1998) *Genes Dev.* **12,** 107–119.
12. Schlaeger, T. M., Qin, Y., Fujiwara, Y., Magram, J. & Sato, T. N. (1995) *Development (Cambridge, U.K.)* **121,** 1089–1098.
13. Xiao, W. & Oefner, P. J. (2001) *Hum. Mutat.* **17,** 439–474.
14. Skopek, T. R., Walker, V. E., Cochrane, J. E., Craft, T. R. & Cariello, N. F. (1992) *Proc. Natl. Acad. Sci. USA* **89,** 7866–7870.
15. Burset, M., Seledtsov, I. A. & Solovyev, V. V. (2001) *Nucleic Acids Res.* **29,** 255–259.
16. Zwijsen, A., van Grunsven, L. A., Bosman, E. A., Collart, C., Nelles, L., Umans, L., Van de Putte, T., Wuytens, G., Huylebroeck, D. & Verschueren, K. (2001) *Mol. Cell. Endocrinol.* **180,** 13–24.
17. Yang, X., Li, C., Xu, X. & Deng, C. (1998) *Proc. Natl. Acad. Sci. USA* **95,** 3667–3672.
18. Beier, D. R. (2000) *Mamm. Genome* **11,** 594–597.
19. Wienholds, E., Schulte-Merker, S., Walderich, B. & Plasterk, R. H. (2002) *Science* **297,** 99–102.
20. Nomura, M. & Li, E. (1998) *Nature* **393,** 786–790.
21. Tremblay, K. D., Hoodless, P. A., Bikoff, E. K. & Robertson, E. J. (2000) *Development (Cambridge, U.K.)* **127,** 3079–3090.
22. Lagna, G., Hata, A., Hemmati-Brivanlou, A. & Massague, J. (1996) *Nature* **383,** 832–836.
23. Zhang, Y., Musci, T. & Derynck, R. (1997) *Curr. Biol.* **7,** 270–276.
24. Maurice, D., Pierreux, C. E., Howell, M., Wilentz, R. E., Owen, M. J. & Hill, C. S. (2001) *J. Biol. Chem.* **276,** 43175–43181.
25. Shi, Y., Hata, A., Lo, R. S., Massagué, J. & Pavletich, N. P. (1997) *Nature* **388,** 87–93.
26. Hata, A., Lo, R. S., Wotton, D., Lagna, G. & Massague, J. (1997) *Nature* **388,** 82–87.
27. Jayaraman, L. & Massague, J. (2000) *J. Biol. Chem.* **275,** 40710–40717.
28. Weinstein, M., Monga, S. P., Liu, Y., Brodie, S. G., Tang, Y., Li, C., Mishra, L. & Deng, C. X. (2001) *Mol. Cell. Biol.* **21,** 5122–5131.
29. Shi, Y., Wang, Y. F., Jayaraman, L., Yang, H., Massague, J. & Pavletich, N. P. (1998) *Cell* **94,** 585–594.
30. Wicks, S. J., Lui, S., Abdel-Wahab, N., Mason, R. M. & Chantry, A. (2000) *Mol. Cell. Biol.* **20,** 8103–8111.
31. Scherer, A. & Graff, J. M. (2000) *J. Biol. Chem.* **275,** 41430–41438.
32. Wisotzkey, R. G., Mehra, A., Sutherland, D. J., Dobens, L. L., Liu, X., Dohrmann, C., Attisano, L. & Raftery, L. A. (1998) *Development (Cambridge, U.K.)* **125,** 1433–1445.
33. de Caestecker, M. P., Yahata, T., Wang, D., Parks, W. T., Huang, S., Hill, C. S., Shioda, T., Roberts, A. B. & Lechleider, R. J. (2000) *J. Biol. Chem.* **275,** 2115–2122.